"ESTAR Measurements during the Southern Great Plains Experiment (SGP99)"

D.M. Le Vine, T.J. Jackson, C.T. Swift, M. Haken and S.Bidwell

Submitted for publication IEEE Trans Geoscience and Remote Sensing

Significant Findings

This paper further supports the evidence that remote sensing of soil moisture from space is possible with passive sensors at L-band and that synthetic aperture radiometry is a viable technology for making this measurement.

ESTAR MEASUREMENTS DURING THE SOUTHERN GREAT PLAINS EXPERIMENT (SGP99)

D.M. Le Vine
Goddard Space Flight Center, Microwave Sensors Branch, Greenbelt, Maryland 20771
Phone: 301-614-5640; FAX: 301-614-5558; email: dmlevine@priam.gsfc.nasa.gov

T.J. Jackson
USDA ARS Hydrology Laboratory, Beltsville, Maryland 20705
Phone: 301-504-8511; FAX: 301-504-8931; email: tjackson@hydrolab.arsusda.gov

C.T. Swift
Department of Electrical Engineering, University of Massachusetts, Amherst, MA 01003
Phone: 413-545-2136; FAX: 413-545-4652; email: klemyk@zonker.ecs.umass.edu

M. Haken, S. Bidwell
Goddard Space Flight Center, Microwave Sensors Branch, Greenbelt, Maryland 20771
Phone: 301-614-5640; FAX: 301-614-5558; email: dmlevine@priam.gsfc.nasa.gov

ABSTRACT

During the Southern Great Plains experiment, the synthetic aperture radiometer, ESTAR, mapped L-band brightness temperature over a swath about 50 km wide and about 300 km long extending west from Oklahoma City to El Reno and north from the Little Washita River watershed to the Kansas border. ESTAR flew on the NASA P-3B Orion aircraft at an altitude of 7.6 km and maps were made on 7 days between July 8-20, 1999. The brightness temperature maps reflect the patterns of soil moisture expected from rainfall and are consistent with values of soil moisture observed at the research sites within the SGP99 study area and with previous measurements in this area. The data add to the resources for hydrologic modeling in this area and are further validation of the technology represented by ESTAR as a potential path to a future mission to map soil moisture globally from space.

ESTAR MEASUREMENTS DURING THE SOUTHERN GREAT PLAINS EXPERIMENT (SGP99)

D.M. Le Vine
Goddard Space Flight Center, Microwave Sensors Branch, Greenbelt, Maryland 20771
Phone: 301-614-5640; FAX: 301-614-5558; email: dmlevine@priam.gsfc.nasa.gov

T.J. Jackson
USDA ARS Hydrology and Remote Sensing Lab, Beltsville, Maryland 20705
Phone: 301-504-8511; FAX: 301-504-8931; email: tjackson@hydrolab.arsusda.gov

C.T. Swift
Department of Electrical Engineering, University of Massachusetts, Amherst, MA 01003
Phone: 413-545-2136; FAX: 413-545-4652; email: klemyk@zonker.ecs.umass.edu

M. Haken, S.W. Bidwell
Goddard Space Flight Center, Microwave Sensors Branch, Greenbelt, Maryland 20771
Phone: 301-614-5640; FAX: 301-614-5558; email: dmlevine@priam.gsfc.nasa.gov

ABSTRACT

During the Southern Great Plains experiment, the synthetic aperture radiometer, ESTAR, mapped L-band brightness temperature over a swath about 50 km wide and about 300 km long extending west from Oklahoma City to El Reno and north from the Little Washita River watershed to the Kansas border. ESTAR flew on the NASA P-3B Orion aircraft at an altitude of 7.6 km and maps were made on 7 days between July 8-20, 1999. The brightness temperature maps reflect the patterns of soil moisture expected from rainfall and are consistent with values of soil moisture observed at the research sites within the SGP99 study area and with previous measurements in this area. The data add to the resources for hydrologic modeling in this area and are further validation of the technology represented by ESTAR as a potential path to a future mission to map soil moisture globally from space.

INTRODUCTION

The Southern Great Plains (SGP) experiment in July, 1999, was one of several recent experiments in Oklahoma designed to gain insight into passive techniques for future remote sensing of soil moisture

from space [1-4]. The participation of ESTAR (Electronically Scanned Thinned Array Radiometer) in these experiments is significant because ESTAR represents an emerging remote sensing technology, called aperture synthesis, with the potential to enable the measurement of soil moisture from space. The measurement of soil moisture from space presents a significant technological challenge because the measurement is optimally done at the long wavelength end of the microwave spectrum. Long wavelengths permit penetration into the soil and mitigate the effects of roughness and vegetation canopy. The window at 1.4 GHz (L-band) set aside for passive use appears to be a good compromise between sensitivity to soil moisture and other issues such as Faraday rotation in the ionosphere and antenna size [5,6]. However, the antennas required in orbit to achieve good spatial resolution are large. For example, to obtain resolution of 10 km at 1.4 GHz would require an antenna more than 15 meters in diameter at 800 km altitude [7].

Although progress is being made on engineering issues associated with putting a large L-band radiometer in space for remote sensing [7-11], the reality in the near term is a sensor at C-band such as the Advanced Microwave Scanning Radiometer (AMSR) scheduled to be flown on the NASA satellite AQUA and the Japanese satellite ADEOS-II. The focus of SGP99 was to provide information on remote sensing of soil moisture at C-band [12] with a connection to previous work at L-band. ESTAR participated to provide soil moisture maps, to provide a bridge to past experiments in this area, and to continue research to validate the technology of aperture synthesis for remote sensing from space. This paper will present examples of the images (maps) made by ESTAR together with a comparison of measured brightness temperature with surface soil moisture.

ESTAR

Aperture synthesis is an interferometric technology designed to address the problem of putting large apertures in space [7,9-10]. ESTAR is a prototype instrument designed to develop the technology for

passive microwave remote sensing and demonstrate its applicability to the measurement of soil moisture. ESTAR is a hybrid that uses real aperture to obtain resolution along track and synthetic aperture to obtain resolution across track [13-14]. ESTAR operates in the L-band window centered at 1.413 GHz reserved for passive use. It images at horizontal polarization and forms an image in the equivalent of a cross-track scan. The scan is actually performed in software as part of the processing that forms the synthesized beam [13]. The synthesized beam has half-power beam width at nadir of about ±4.5 degrees; however, smoothing generally is employed in the ESTAR images to reduce the sidelobes. The beam width of the smoothed beam is about ±6.5 degrees at nadir. This corresponds to a resolution of about 1.7 km at an altitude of 7.6 km.

The 1999 Southern Great Plains experiment (SGP99) was designed to gain insight into the performance of instruments that will be available in the near future for remote sensing of soil moisture from space. In particular, passive remote sensing data at C-band will soon be available from space with instruments such as the Advanced Microwave Scanning Radiometer (AMSR). Experience with remote sensing of soil moisture at L-band has been obtained using airborne sensors [1,2,15-16] but little data exists on the retrieval of soil moisture from space using C-band. In the more distant future, remote sensing at L-band will be possible from space when the Soil Moisture and Ocean Salinity (SMOS) mission being developed in Europe for the European Space Agency (ESA) is launched [10,17-18]. The L-band radiometer on SMOS will be a synthetic aperture radiometer, the same technology as employed in ESTAR, but with antennas arranged in a "Y" configuration [17-18].

ESTAR has mapped soil moisture in the vicinity of the SGP99 study area in the past. ESTAR mapped the Little Washita watershed in 1992 [1,13] and mapped the current study area in 1997 during an experiment called SGP97 [2]. The goal for ESTAR during SGP99 was to provide data to study soil

moisture retrieval at L-band, to provide continuity with the previous experiments in this area and to provide an overview of soil moisture in the study area for comparison with observations at C-band.

EXPERIMENT

The SGP99 experiment took place in Oklahoma, west of Oklahoma City at the same site used in SGP97 (see Figures 1-2 in [2]). This area is among the best instrumented sites in the world for monitoring soil moisture. It includes the United States Department of Agriculture (USDA) Agricultural Research Service (ARS) facilities within the Little Washita River watershed (LW), the ARS grass land research facility at El Reno (ER) and the ARM CART Central Facility (CF) near Lamont, OK. In general, this is an area of gently rolling hills with a transition from grasses in the south to winter wheat in the north. Specifically, the Little Washita River watershed (south) is mostly rangeland and pasture (63%) with the remainder being mostly winter wheat with a mixture of other crops. The ARS facility at El Reno (ER) consists of grasslands that range from winter wheat to natural prairie. The fields selected for soil moisture sampling at the Central Facility (CF) are a mixture of grass and winter wheat.

Figure 1 shows the lines flown by ESTAR during the Southern Great Plains experiment. The flight plan consisted of 4 parallel straight lines extending from the Little Washita Watershed in the south to the Kansas border at the northern end. Two short east-west lines in the vicinity of Oklahoma City (OKC) were added to compensate for RFI experienced by ESTAR when it flew in a north-south direction past Oklahoma City. Orienting the instrument in an east-west direction uses the along-track antenna pattern (real aperture) of the ESTAR antennas to reduce the effects of RFI coming from OKC. These additional lines were necessary to insure coverage of the ground sites at El Reno. All of the flight lines were at an altitude of 7.6 km (25 kft.). The flight lines were flown in numerical order and in alternate directions, beginning at the northern end of line 1 (flying north-to-south) and then continuing with the southern end of line 2 and flying south-to-north. Line 5 was flown east-to-west and line 6 was flown west-to-east. The

flight plan also included a low altitude pass (300 m) over Lake Kaw located at about latitude 36.7 N and just east of line 7. This provided a fresh water source for calibration. It was flown at the end of the mission after completion of line 7 on the return to OKC.

ESTAR arrived in Oklahoma on July 7, 1999 and flew mapping missions on July 8, 9, 11, 14, 15, 19 and 20. The aircraft was down on July 10 by design and was down again on July 12-13 and 16-18 with mechanical problems. ESTAR also experienced some problems during the experiment. The zero baseline (total power) channel was lost on portions of July 9 and all of July 11 due to failure of a voltage regulator caused by metal fatigue. There were also intermittent problems with the data system that caused some small loss of data. ESTAR has additional total power channels that can be used as backup for the failed zero spacing channel. These are noisier and not as well calibrated as the noise injection radiometer normally used for this data. They were used to reconstruct the ESTAR data for July 11 for use in the images but they were not used in the quantitative comparison with surface measurements. A summary of the mission is given in Table I. The period of the experiment (July 8-20) was largely dry with the exception of a large storm on night of July 10.

RESULTS

Figure 2 shows the ESTAR brightness temperature map for July 15. This is typical of the maps made by ESTAR during SGP99 and is representative of a study area that was moist to the northwest (cool colors) and very dry in the extreme southeast (warm colors). The previous major rainfall occurred several days earlier on the evening of July 10 but largely missed the southeast corner of the study area. The map is superimposed on the major waterways in the area. These are the Arkansas River in the north, the Cimarron River in the middle and the Canadian River south of Oklahoma City (triangle labeled OKC). Note Lake Kaw in the northeast corner of the map. This is where the water calibration of ESTAR was done after each day's flight. Evidence of the four north-south lines can be seen at the top and bottom of

the image in Figure 2. The east-west lines over El Reno are evident in the indentations in the map at about 35.5 N latitude. The dark spots in the southwest corner of the map are small bodies of water (cold brightness temperatures). The rectangles indicate the sites where measurements of soil moisture were made (discussion to follow below).

Making ESTAR brightness temperature maps involves several steps. The data is filtered to remove spurious points such as spikes due to radio frequency interference (RFI) and then the raw voltages are calibrated. ESTAR uses internal noise diodes to maintain stability and correct for phase and gain variations [13]; absolute calibration is achieved using "warm" and "cold" loads in a manner similar to that of conventional radiometers. The warm load used by ESTAR is a blackbody. A box of absorber is observed on the ground before and after each flight and the anechoic chamber at Goddard is used before and after each mission. The cold load is a body of water observed in flight. In SGP99 the Atlantic Ocean was observed before and after the mission and Lake Kaw (near Ponca City) was used while in Oklahoma. For the data presented here, absolute calibration was done using data collected over the Atlantic Ocean near the NASA Wallops Flight Center after the return from Oklahoma. The ocean calibrations done before and after the mission appear to be superior in that they were less contaminated by land than the lake data. Also, a ship was at the ocean site to provide accurate measurements of salinity and temperature. The blackbody data collected in the anechoic chamber at the Goddard Space Flight Center was used here. In developing calibration coefficients, a correction is made for atmospheric and cosmic background radiation in data collected over the ocean. But in the results presented in the figures to follow no correction has been made for the physical temperature of the surface nor for down welling or upwelling radiation.

Given the calibration, the next step is to generate images. First the transformation is made from Fourier space to brightness temperature as a function of incidence angle. This is done separately for each

cross track scan using the impulse response of the instrument as measured before the experiment in the laboratory [13,19]. Each scan is geolocated using GPS and topographic maps to indicate position and using the aircraft data system to indicate aircraft attitude (pitch, roll and yaw). Next, the data are corrected for incidence angle. This is done by averaging along track to determine the mean change with incidence angle and correcting for the measured roll-off (brightness temperature at horizontal polarization decreases with incidence angle). The roll-off correction also removes artifacts such as a Gibb's phenomena which often remain from the original image reconstruction. Next, each geolocated and corrected ESTAR cross track scan is mapped to a cartesian grid on the surface. The brightness temperatures in any boxes in the grid that were mapped more than once (e.g. by adjacent flight lines) are averaged. Finally, a linear interpolation is done to fill small gaps left, for example, from the removal of RFI. Large gaps, such as are evident at the top and bottom of Figure 2 and adjacent to Oklahoma City, are not smoothed.

Figure 3 is a sequence of all the images made in SGP99 (July 8, 9, 11, 14, 15, 19 and 20). The images on July 8 and 9 were made at the beginning of the experiment and are representative of a relatively dry study area. A large rain event (over 100 mm of rain at El Reno) occurred on the evening of July 10. Most of the study area received rain with the exception of the southeast corner. The effect of this exception can be seen in the brightness temperature in the lower right-hand corner of the images which continues to increase from July 9 to 20. In contrast, the remainder of each image shows a decrease in brightness temperature after the rain event. There was no further rain during the experiment and this is reflected in the maps for July 14-20 which show a progressive increase in brightness temperature indicative of drying in the study area. In the map for July 20 the moisture associated with the network of rivers is evident. Also, evidence of the Cimarron River and Canadian River can be seen in the maps for July 9 and 15 (near the center).

To obtain a more quantitative evaluation of the images, a comparison has been made with soil moisture measured at several sites within the area mapped by ESTAR. From north-to-south these sites are the Central Facility (CF), the USDA research facility at El Reno (ER) and the Little Washita watershed (LW). The rectangles in Figure 2 represent the outer perimeter of the sites where sampling was done. The actual sampling was done in fields distributed within the area indicated by the boxes. Given that the resolution of the microwave measurements (about 1 km) was comparable to the size of the fields sampled, it would be unreliable to make a field by field comparison. Hence, a comparison has been made of the average value of ESTAR brightness temperature within each box with the average value of all the soil moisture samples taken that day within that box. As can be seen in the box around the Little Washita River watershed (bottom box in Figure 2), there is some variation within the area to be averaged. This variation reflects real features within this area (differences in soil moisture, soil properties or land cover) and an attempt was made in the distribution of surface sampling to represent these differences. The average brightness temperatures were checked and averages with a large standard deviation (greater than 7 K) were eliminated. Also, boxes with few ESTAR observations were eliminated. Finally, the data for July 11, which used the substitute zero-spacing channel, were not used since this represents an unvalidated algorithm.

The results are shown in Figures 4-7. Figure 4 is a scatter plot showing the average brightness temperature plotted against average soil moisture for each of the three areas. Notice that, with the exception of the two points for which $T_B < 260K$ (recorded on July 15 at the CF and ER sites), the range of soil moisture encountered during the experiment was small and confined to relatively dry soil. Unfortunately, the effect of the rainfall event on July10 is not represented in the data. The rain event itself was missed due to equipment problems (see Table I) and reliable data were not collected until July 14, four days after the storm.

Figures 5-7 show a comparison of the data collected in 1999 with data collected under very similar conditions during the Southern Great Plains experiment in 1997 (SGP97). The flight plan for the ESTAR instrument and the surface sampling were similar in SGP97. Lake Kaw and post flight blackbody measurements were used for calibration in 1997. Five lake overflights were selected which appeared to have minimum contamination by land. The five scenes gave slightly different brightness temperatures, and it was decided to use the average value obtained from the five cases for this comparison. Again, the data are raw brightness temperature with no correction for physical temperature of the surface nor for upwelling or downwelling background radiation. These data are plotted with the data from SGP99 as solid symbols in Figures 5-7.

Figure 5 shows the data collected at the Central Facility (CF). The open squares are data collected during SGP99 and the closed squares are data for SGP97. The data plotted here are averages for each day. The ESTAR brightness temperature is the average for each of the boxes shown in Figure 2 for each day. The soil moisture (volumetric soil moisture) is the average of all the measurements made on a given day within each of the respective boxes. The range of soil moisture encountered in SGP99 is clearly less in SGP97; however, the trend (slope) is similar. The extreme values observed in 1999 are consistent with the dry conditions encountered during SGP99.

Figure 6 shows the scatter plot of brightness temperature against soil moisture for the Little Washita River watershed (LW). The open circles are the average values for each day obtained during SGP99 and the closed circles are for SGP97. Again, notice that the trends are consistent and notice the drier conditions in 1999.

Figure 7 shows the data collected at the El Reno site (ER). The open triangles are daily averages for SGP99 and the closed triangles are for SGP97. Again, the drier extremes that were encountered during SGP99 are evident. But, in this case, there appears to be a difference in the trend (T_B vs soil

moisture) for the SGP99 and SGP97 data. The reason for this difference is not clear. However, the trend is clearly dependent upon one point (the open triangle with $T_B \approx 255K$, observed on July 15).

With the exception of three data, the standard deviation of the ESTAR averages in SGP99 is 3-5 K. The three points (two in the LW and one in ER) had standard deviations of 6-7. One point on July 14 in ER was dropped because of a very high standard deviation (9K). The standard deviation is combination of instrument noise and variations of surface characteristics within the sites defined by the boxes in Figure 2. The larger standard deviations tended to be associated with the Little Washita watershed (LW) and the smallest (3K) with the Central Facility (CF), which is consistent with the variation of land surface parameters at the sites that influence T_B. Finally, in 1999, there were no data for the Central Facility for July 14 and there were no ESTAR data over El Reno on July 8.

CONCLUSIONS

The L-band measurements of brightness temperature made by ESTAR during the Southern Great Plains experiment in 1999 reflect the spatial and temporal patterns of soil moisture within the study area. The data compare well with previous observations made earlier during SGP97 under very similar conditions. The data presented here are raw brightness temperature. The effects of surface temperature and background radiation have not been removed. Since SGP99 and SGP97 were conducted under very similar conditions (time of day, time of year, air temperature) it is felt that such a comparison is justified. However, for more extensive comparison, emissivity should be used.

ACKNOWLEDGMENT

Support for this research was provided by NASA from the Land Hydrology Program, the EOS Interdisciplinary Science Program, and by the EOS Aqua AMSR program. The authors would also like to acknowledge crew of the P-3 Orion and the numerous scientists that supported ground data collection during this experiment.

REFERENCES

[1] T.J. Jackson, D. M. Le Vine, C.T. Swift, T.J. Schmugge and F.R. Schiebe, "Large area mapping of soil moisture using the ESTAR passive microwave radiometer in Washita-92", *Remote Sens. Environ.*, Vol. 53, pp. 27-37, 1995

[2] T.J. Jackson, D.M. Le Vine, A.Y. Hsu, A. Oldak, P.J. Starks, C.T. Swift, J.D. Isham and M. Haken, "Soil moisture mapping at regional scales using microwave radiometry: The Southern Great Plains hydrology experiment", *IEEE Trans. Geosci. Remote Sensing*, Vol. 37, (#5), pp. 2136-2151, 1999.

[3] T.J. Jackson and D.M. Le Vine, "Mapping Surface Soil Moisture Using an Aircraft-based Passive Microwave Instrument: Algorithm and Example", *J. Hydrology*, Vol. 184, pp. 85-99, 1996.

[4] D.M. Le Vine et al, "Passive microwave remote sensing with the synthetic aperture radiometer, ESTAR, during the Southern Great Plains experiment, *Proc. IGARSS98*, Vol. 5, pp. 2606-2608, Seattle, WA, July, 1998.

[5] D.M. Le Vine and S. Abraham, "Faraday rotation and passive microwave remote sensing of soil moisture from space", *Microwave Radiometry and Remote Sensing of the Earth's Surface and Atmosphere*, The Netherlands, VSP, P. Pampaloni and S. Paloscia, Eds., pp. 89-96, 2000.

[6] C.T. Swift, and R.E. McIntosh, "Considerations for microwave remote sensing of ocean-surface salinity", *IEEE Trans. Geosci. Remote Sensing*, Vol 21 (#4), pp. 480-491, 1983.

[7] E.G. Njoku, W.J. Wilson, S.H. Yueh and Y. Rahmat-Samii, "A large-antenna microwave radiometer-scatterometer concept for ocean salinity and soil moisture sensing", *IEEE Trans. Geosci. Remote Sensing*, Vol 38(#6), 480-491, 2000.

[8] D. M. Le Vine et al., "A multifrequency microwave radiometer of the future", *IEEE Trans. Geosci. Remote Sensing*, Vol. 27 (#2) pp. 193-199, March, 1989.

[9] C.T. Swift, D.M. Le Vine and C.S. Ruf, "Aperture Synthesis concept in microwave remote sensing of

the earth", *IEEE Trans on Microwave Theory and Tech.*, Vol. 39 (#12), pp. 1931-1935, 1991.

[10] M. Martin-Neira and J.M. Goutoule, "MIRAS-A two dimensional aperture synthesis radiometer for soil-moisture and ocean-salinity observations", *ESA Bull. European Space Agency*, Vol. 92, pp. 95-104, 1997.

[11] D.M. Le Vine, J.B. Zaitzeff, et al., "Sea surface salinity: Toward an operational remote sensing system", *Satellites, Oceanography and Society*, The Netherlands, Elsevier Science, D. Halpern, Ed., Chap. 19, pp. 321-335, 2000.

[12] T. J. Jackson and A. Y. Hsu, "Soil moisture and TRMM microwave imager relationships in the Southern Great Plains 1999 (SGP99) experiment ," *IEEE Trans. Geosci. Remote Sensing*, this issue.

[13] D.M. Le Vine, A.J. Griffis, C.T. Swift and T.J. Jackson, "ESTAR: A synthetic aperture microwave radiometer for remote sensing applications", *IEEE Proc.*, Vol. 82 (#12), pp. 1787-1801, Dec, 1994.

[14] D. M. Le Vine et al., "Initial results in the development of a synthetic aperture microwave radiometer," *IEEE Trans. Geosci. & Remote Sens.* Vol. 28 (#4), pp. 614-619, 1990.

[15] T.J. Schmugge, T.J. Jackson, W.P. Kustas, J.R. Wang, "Passive microwave remote sensing of soil moisture: Results from HAPEX, FIFE and MONSOON'90", *ISPRS J. Photo. Remote Sensing*, Vol. 47, pp. 127-134, 1992.

[16] T.J. Schmugge, J. R. Wang and G. Asrar, "Results from the push broom microwave radiometer flights over the Konza prairie in 1985", *IEEE Trans. Geosci. Remote Sensing*, Vol. 26, pp 590-596, 1988.

[17] D.M. Le Vine, "Synthetic aperture radiometer systems", *IEEE Trans. MTT*, Vol. 47 (#12), pp. 2228-2236, Dec., 1999.

[18] Y. H. Kerr, Waldteufel P., Wigneron J. P., Martinuzzi J. M., Lazard B., Goutoule J. M. and Lannes A., "The soil moisture and ocean salinity mission: An overview", *Microwave Radiometry & Remote*

sensing of the Earth's Surface and Atmosphere, VSP, The Netherlands, P. Pampaloni and S. Paloscia, Ed., pp 467-475, 2000.

[19] A.B. Tanner, "Aperture synthesis for passive microwave remote sensing: The electronically scanned thinned array radiometer", *Ph-D dissertation*, Dept of Elec. Engin, University of Massachusetts, Feb. 1990.

TABLE I: FLIGHT SUMMARY

DATE JULY, 1999	FLIGHT LINE	WATER CAL	BB TEMP K	COMMENT
7	Transit	Ocean		WFF → OKC
8	Nominal	Lake Kaw	95	
9	Nominal	------	95	NF problem (line 3 to end)
10				Rain (PM); Scheduled down day
11	Nominal			NF failed
12				Down: P-3 window
13				Down: P-3 window
14	Nominal	Lake Kaw	91.5	
15	Nominal	Lake Kaw	87	
16				Down: P-3 wing
17				Down: P-3 wing
18				Down: P-3 wing
19	Nominal	Lake Kaw	90	
20	Nominal	Lake Kaw		
21	Transit			OKC → WFF

FIGURE CAPTIONS

Figure 1: The ESTAR flight lines during SGP99. The lines were flown in numerical order beginning in the northwest corner with line 1 which was flown north-to-south. Next was line 2 which was flown south-to-north.

Figure 2: ESTAR image for July 15, 1999. The rivers shown are from top to bottom, the Arkansas River, the Cimarron River and the Canadian River. The rectangles indicate the surface sites where measurements of soil moisture were made. They are (top to bottom): Central Facility (CF), the ARS site at El Reno (ER) and the Little Washita River watershed (LW). The rectangles are the areas used to compute the average ESTAR brightness temperature.

Figure 3: Sequence of ESTAR images from SGP99. Significant rain occurred on the evening of July 10.

Figure 4: Scatter plot showing average ESTAR brightness temperature and average soil moisture for each of the three sites during SGP99 (CF = square; LW = circle; ER = triangle)

Figure 5: Scatter plot showing average ESTAR brightness temperature and average soil moisture for the Central Facility. Open symbols are for SGP99 and closed symbols are data from SGP97.

Figure 6: Scatter plot showing average ESTAR brightness temperature and average soil moisture for the Little Washita River watershed. Open symbols are for SGP99 and closed symbols are data from SGP97.

Figure 7: Scatter plot showing average ESTAR brightness temperature and average soil moisture for the site at El Reno. Open symbols are for SGP99 and closed symbols are data from SGP97.

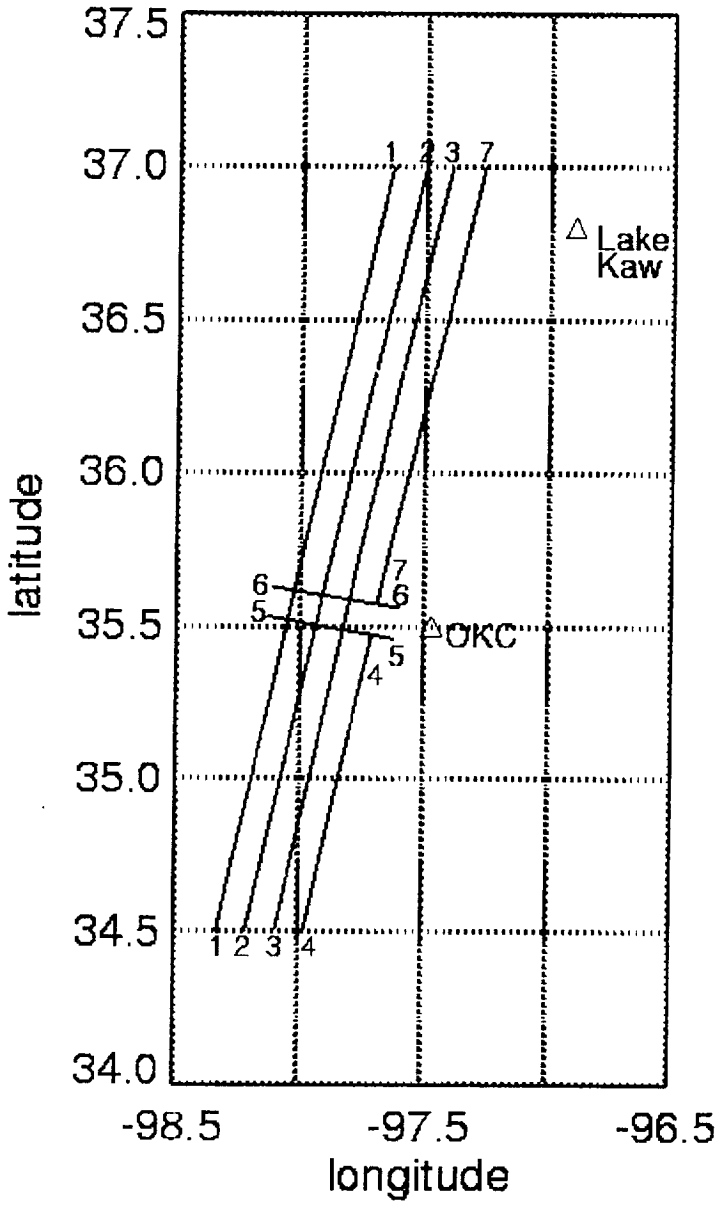

Figure 1: The ESTAR flight lines during SGP99. The lines were flown in numerical order beginning in the northwest corner with line 1 which was flown north-to-south. Next was line 2 which was flown south-to-north.

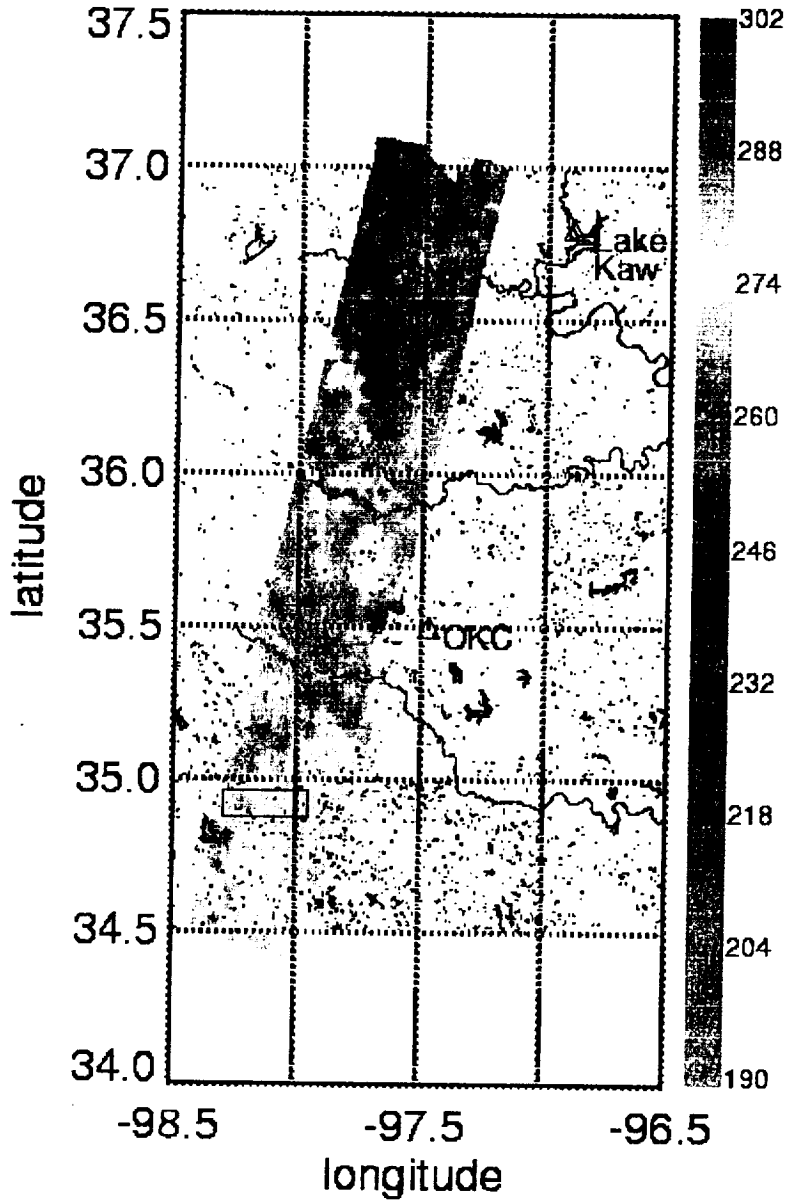

Figure 2: Figure 2: ESTAR image for July 15, 1999. The rivers shown are from top to bottom, the Arkansas River, the Cimarron River and the Canadian River. The rectangles indicate the surface sites where measurements of soil moisture were made. They are (top to bottom): Central Facility (CF), the ARS site at El Reno (ER) and the Little Washita River watershed (LW). The rectangles are the areas used to compute the average ESTAR brightness temperature.

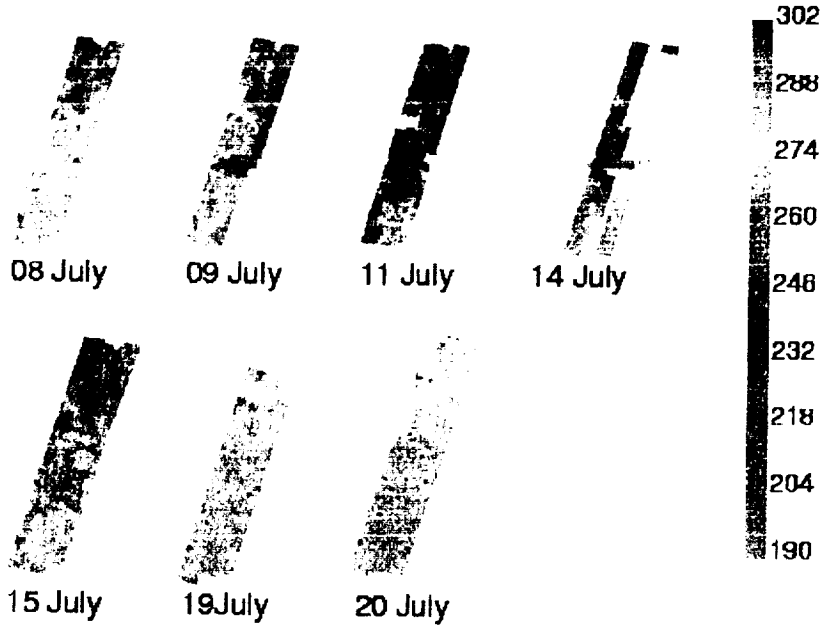

Figure 3: Sequence of ESTAR images from SGP99. Significant ran occurred on the evening of July 10.

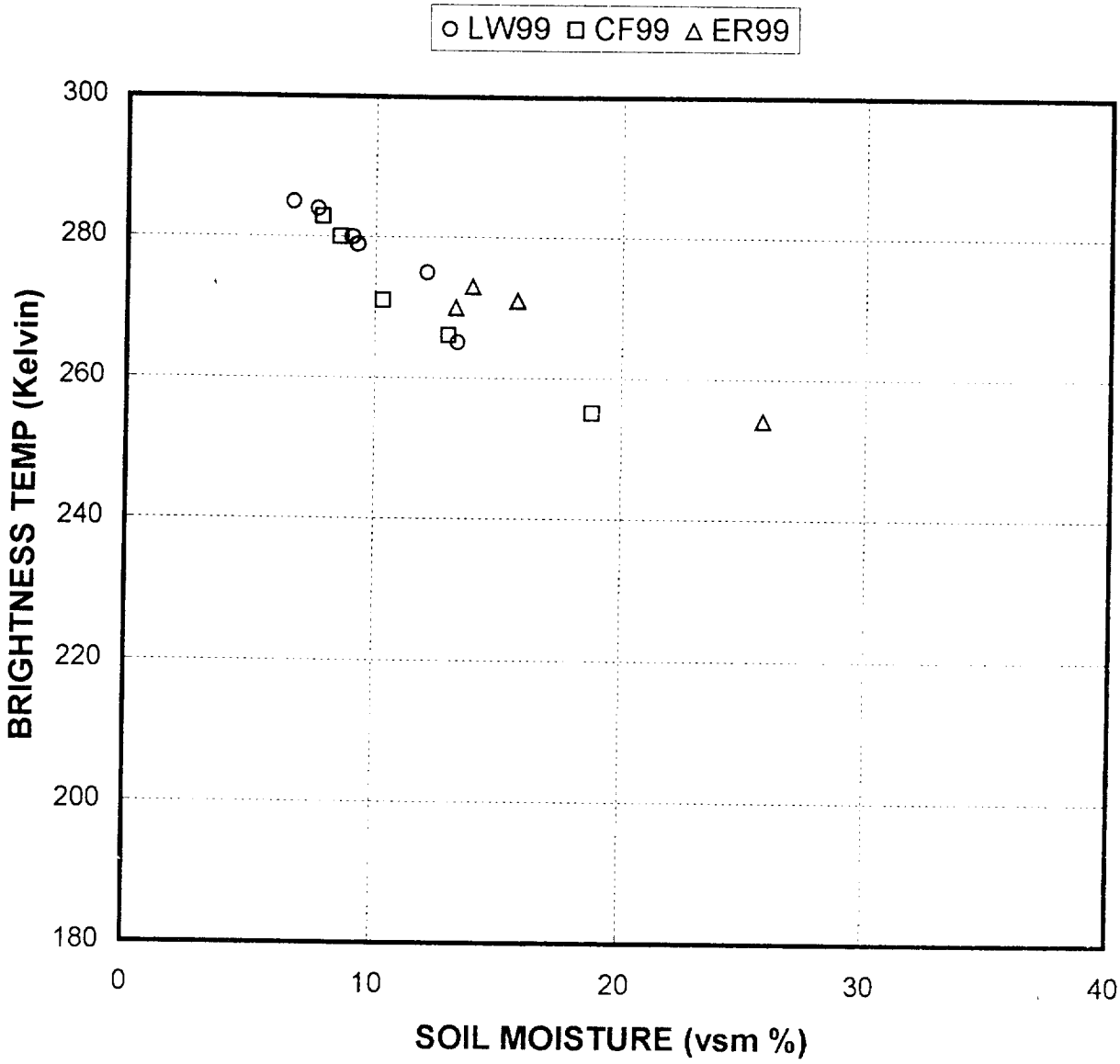

Figure 4: Scatter plot showing average ESTAR brightness temperature and average soil moisture for each of the three sites during SGP99 (CF = square; LW = circle; ER = triangle).

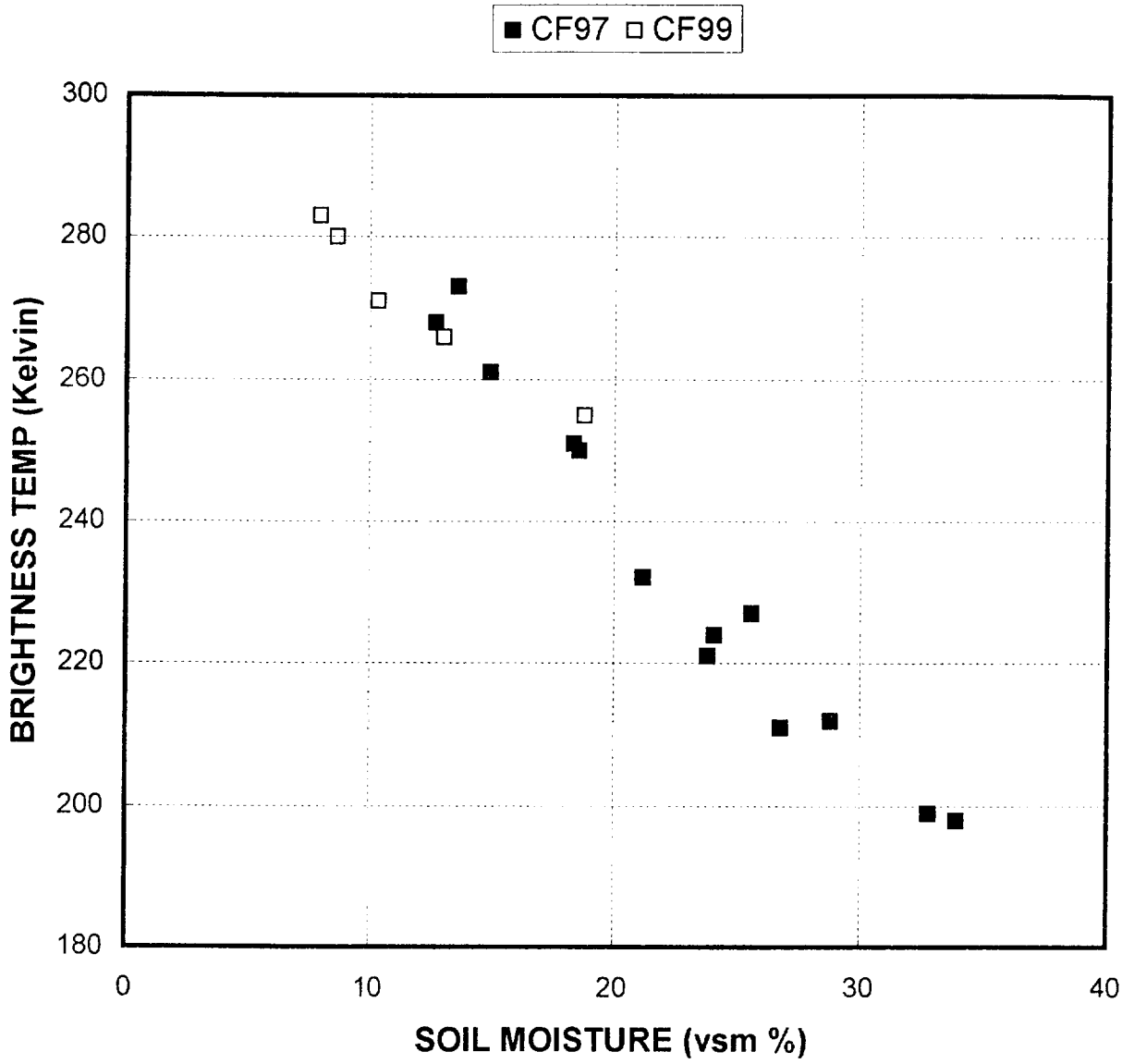

Figure 5: Scatter plot showing average ESTAR brightness temperature and average soil moisture for the Central Facility. Open symbols are for SGP99 and closed symbols are for SGP97.

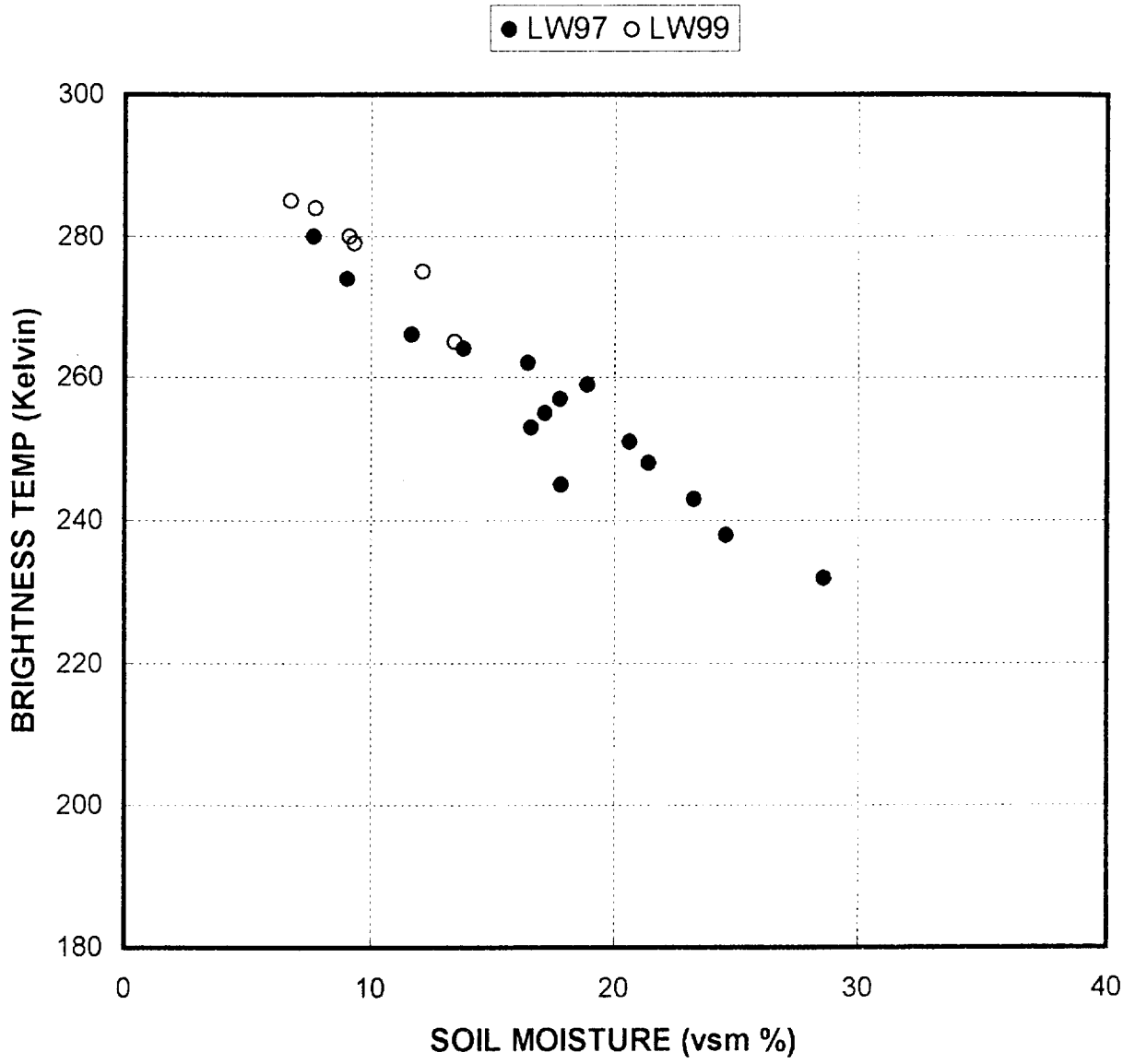

Figure 6: Scatter plot showing average ESTAR brightness temperature and average soil moisture for the Little Washita River watershed. Open symbols are for SGP99 and closed symbols are for SGP97.

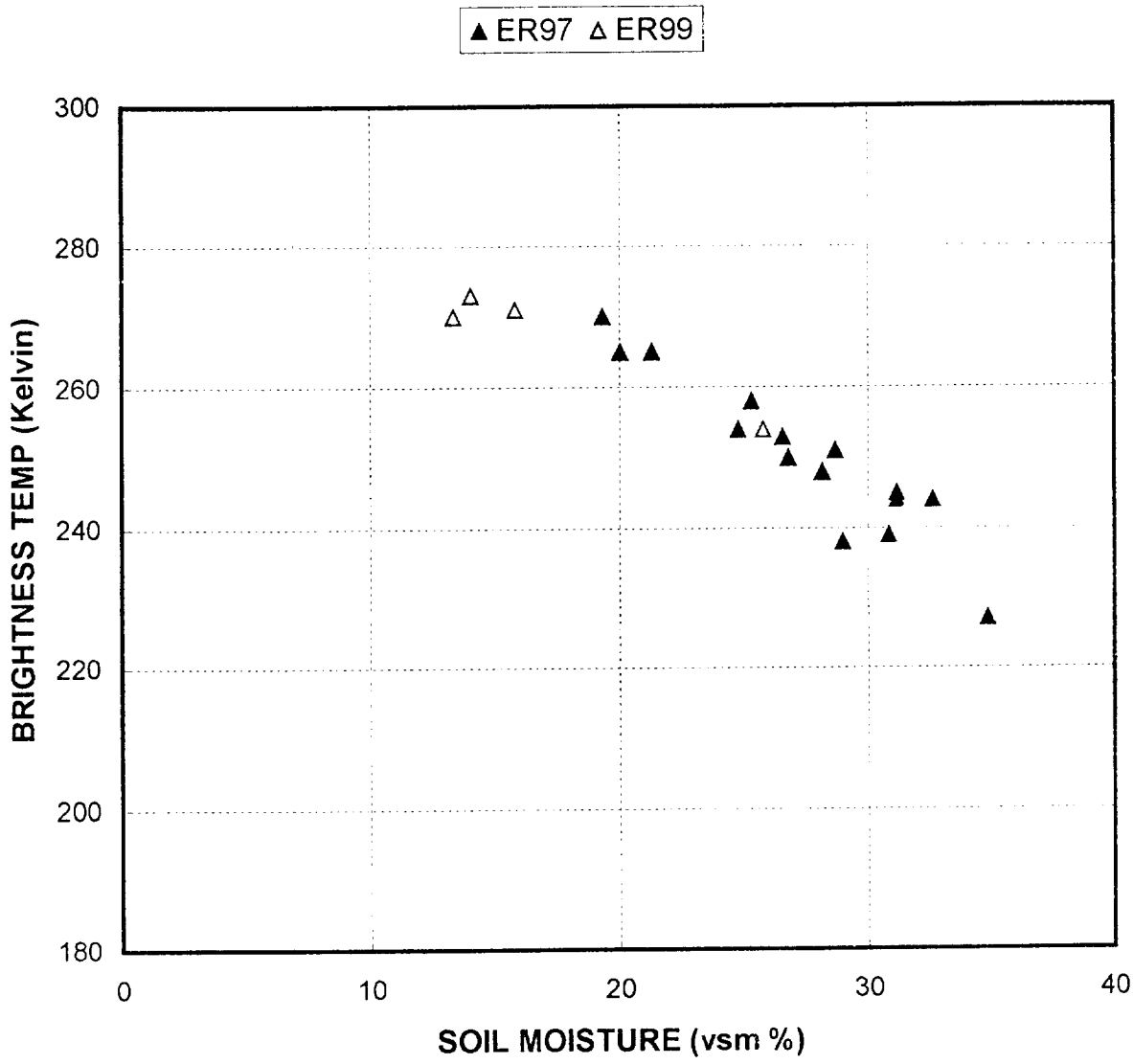

Figure 7: Scatter plot showing average ESTAR brightness temperature and average soil moisture for the site at El Reno. Open symbols are for SGP99 and closed symbols are data from SGP97.